

Thermomechanical Constitution of Shape Memory Polymer

Z.D. Wang¹, D.F Li¹

Summary

The thermo-mechanical constitution of shape memory polymers (SMPs) is critical for predicting their deformation and recovery characteristics under different constraints. In this study, a new, physical-based, temperature and time-dependent constitutive model is proposed for simulating the thermomechanical response of SMPs. The deformation mechanisms of shape fix and shape recovery are analyzed. Different models are compared to compare strain and stress recovery responses with the experimental results.

keywords: Shape memory polymer; Thermomechanical constitution; Temperature

Introduction

Shape memory polymers (SMPs) possess the ability to store and recover large strains by applying a prescribed thermomechanical cycle. The thermal-induced storage and recovery mechanisms have been described in molecular structure as shown in Fig. 1 [1]. A SMP has characteristics of amorphous state with appropriate cross-linking density. At temperatures well above T_g , the amorphous segments are flexible and the polymer is in the rubber state (initial state). More than several hundred percent of elastic strains can be applied through large-scale conformational changes in this state.

When applying a specified initial deformation on the polymer and cooling down the temperature well below T_g , the amorphous segments is fixed and large-scale conformational changes become impossible. The pre-deformed strain can be basically sustained even if the applied load was removed (temporary state). When reheating the temperatures to be above T_g , the amorphous segments becomes flexible again. The material is forced back to its permanent shape (initial state) due to micro-Brownian thermal motion.

SMPs have many advantages over shape memory alloys and ceramic in easy processing, low density (1.0-1.3 g/cm³), high shape recovery (maximum shape recovery ratio more than 400%), and low manufacturing cost. Their potential ap-

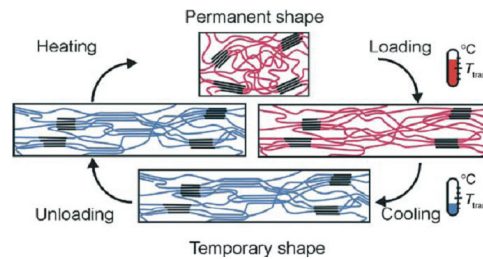


Figure 1: Deformation mechanism of SMPs

¹Institute of Mechanics, School of Civil Engineering, Beijing Jiao-Tong University, Beijing, 100044, China

plications are gradually receiving much attention. For example, the biodegradable SMPs are useful in medicine including wound sutures, filling and sealing cranial aneurysms [2-4]. continuous-fiber-reinforced shape memory composites have developed substantial interest in future deployable space-structure industry [5-7]. Several investigators have exploited the SMP-based MEMS with functions such as gripping or releasing therapeutic medical devices within blood vessels [8-9].

The thermomechanical constitution of a SMP is critical for predicting its deformation and recovery under different constraints. Some works have been done in this field. For example, Bhattacharyya and Tobusi proposed a rheological constitutive model [10], which did not consider the different strain storage and release mechanisms at the molecular level and thus has limited predictive power. Rao delineated the modeling of SMP into four parts and addressed these parts separately [11] by using a framework that was developed for studying crystallization in Polymers [12,13]. Liu et al developed a small-strain constitutive model [14] that can be used to explain the thermomechanical cyclic experiments. However, so far the previous models are rate-independent, and the frozen fractions of pre-strain and thermal strain are not differentiated. Moreover, the simple mix law in predicting the equivalent Young's modulus is not suitable when considering the great difference of the frozen and active Young's modulus. In this study, a new thermomechanical model was proposed avoiding such deficiencies. The modeling results were verified by the available experimental results.

Thermomechanical constitutive model for SMPs

Frozen fraction

In a three-dimensional mode, the frozen fraction and the active fraction satisfy

$$\Phi_f(T) = \frac{V_f(T)}{V}, \quad \Phi_a(T) = \frac{V_a(T)}{V}, \quad \Phi_f(T) + \Phi_a(T) = 1, \quad (1)$$

where V is the total volume of the polymer, V_f the volume of the frozen phase and V_a the volume of the active phase.

The shape memory and recovery characteristics are determined by the frozen volume fraction, which is a critical parameter. Liu et al. [14] assumed the frozen volume fraction as a phenomenological function of the temperature with two variables, c_f and n

$$\Phi_f = 1 - \frac{1}{1 + c_f (T_h - T)^n}, \quad (2)$$

where T_h is the pre-deformation temperature.

It is clear that there is a significant deficiency in Eq. (2). The pre-deformation temperature is not a material variable. Different researchers ever gave the different pre-deformation temperature. In Liu et al's experiment, $T_h = T_g + 20K$, where T_g

denotes the glass transition temperature of SMPs. Tobushi et al. [16], however, gave the relationship of $T_h = T_g + 15K$.

Considering the significant change of material's parameters in the glass change region, $T_l \leq T \leq T_h$, Tobushi et al. [15] simply assumed that all the material parameters (e.g. Young's modulus, viscosity and yielding stress) could be generally expressed by an exponential function of the temperature

$$x = x_g \exp \left[a \left(\frac{T_g}{T} - 1 \right) \right], \quad (T_l \leq T \leq T_h) \quad (3)$$

where x_g is the value of the general material parameter x at $T = T_g$, T_l is the strain storage temperature. It is clear that Eq. (3) can only give a rough explanation about the shape memory and recovery characteristics of SMPs. The predictive power is limited. Therefore, a more convinced and physical-based expression of the frozen fraction should be given.

Fig. 2 shows the typical experimental results about the frozen strain of SMPs as a function of the temperature. The frozen transition process focuses on a small transition zone.

As the temperature is higher than a critical value, no frozen strain exists. As the temperature is lower than the critical value, the frozen strain increases quickly and soon goes to a saturation value close to the pre-strain. This behavior is very similar to the crystallization process of asemi-crystallization polymer. Hence, the crystallization theory can be applied to simulate the frozen process of SMPs. According to the Avrami equation [16] modified by Ozawa [17], the frozen process of SMPs is given by

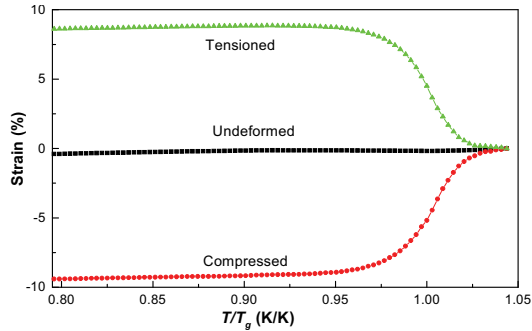


Figure 2: Frozen strains vs. temperatures

$$\Phi_f(T, \beta) = \alpha \exp[-F(T)/\beta^n], \quad (4)$$

where α is the final frozen fraction. $F(T)$ is a function of the temperature, which can be normalized by the glass transition temperature T_g as $F(T) = (T_g/T)^m$, β and n are the cooling rate and Avrami exponent, respectively.

Eq. (4) indicates that the frozen process of SMPs is rate-dependent. Non-isothermal cooling will lead to lower temperature than isothermal cooling to receive the same frozen fraction. For isothermal increase or decrease the temperature, Eq.

(5) can be further simplified as

$$\Phi_f(T) = \alpha \exp[-K (T_g/T)^m], \quad (5)$$

where $K = 1/\beta^n$ is a material's constant. As a kind of polymers, the frozen deformation is not an instantaneous response, but a time-consuming process. The transition temperatures should be different when cooling and heating at a constant rate. Consequently the frozen fractions at a constant cooling/heating rate, β , can be expressed as Eqs. (6) and (7), respectively:

$$\Phi_f(T) = \alpha \exp[-K (T_g/T + \tau)^m], \quad (6)$$

$$\Phi_f(T) = \alpha \exp[-K (T_g/T - \tau)^m], \quad (7)$$

where τ is a normalized retardant time, which is dependent on the microstructure of SMPs (e.g. cross-linking density).

Effective compliance and stiffness tensors

SMPs can be regarded as a two-phase composite in the frozen transition region. The active phase and the frozen phase are matrix and reinforcement, respectively. Their volume fractions are temperature-dependent. With decreasing the temperature, the volume fraction of the matrix (active phase) is decreased and that of the reinforcement (frozen phase) is increased. As the temperature is lower than the lower critical value of the frozen transition region, the volume fraction of the frozen phase is much higher. Hence the Mori-Tanaka approach [18] was used to predict the effective elastic properties of SMPs because both matrix/reinforcement action and reinforcement/reinforcement action are considered in this method. Following this approach, the overall elastic-stiffness tensor of the composite is

$$\tilde{\mathbf{L}} = \mathbf{L}_a (\mathbf{I} + \Phi_f \mathbf{A})^{-1}, \quad (8)$$

$$\mathbf{A} = \{\mathbf{L}_a + (\mathbf{L}_f - \mathbf{L}_a)\} [\Phi_f \mathbf{I} + (1 - \Phi_f) \mathbf{S}]^{-1} (\mathbf{L}_a - \mathbf{L}_f),$$

where the boldface terms indicate tensor quantities, \mathbf{L}_a and \mathbf{L}_f are respectively the stiffness tensors of the active phase and frozen phase, \mathbf{I} is the identity tensor, \mathbf{S} is the Eshelby tensor [19]. For spherical effective particle and an isotropic matrix, the components of the Eshelby tensor can be simplified as [20]

$$S_{1111} = S_{2222} = S_{3333} = \frac{7 - 5\nu}{15(1 - \nu)},$$

$$S_{1122} = S_{2233} = S_{3311} = S_{1133} = S_{2211} = S_{3322} = \frac{5\nu - 1}{15(1 - \nu)},$$

$$S_{1212} = S_{2323} = S_{3131} = \frac{4 - 5\nu}{15(1 - \nu)}, \quad (9)$$

where ν is the Poisson's ratio of the active phase. For SMPs studied here, both active and frozen phases are assumed to be isotropically thermoelastic, and the frozen phase is taken to be spheroids of identical shape, to be perfectly bonded to the active phase. Hence it is evident from Eqs. (7)-(9) that the composite stiffness tensor is isotropic.

Thermomechanical constitution

The following relation can be received when a pre-strain applied on SMPs in the glass transition region

$$\boldsymbol{\varepsilon} = \boldsymbol{\varepsilon}^{pre} + \boldsymbol{\varepsilon}^T = \Phi_f \boldsymbol{\varepsilon}_f + (1 - \Phi_f) \boldsymbol{\varepsilon}_a, \quad \boldsymbol{\varepsilon}_f = \boldsymbol{\varepsilon}_f^M + \boldsymbol{\varepsilon}_f^T, \quad \boldsymbol{\varepsilon}_a = \boldsymbol{\varepsilon}_a^M + \boldsymbol{\varepsilon}_a^T, \quad (10)$$

where $\boldsymbol{\varepsilon}^{pre}$ and $\boldsymbol{\varepsilon}^T$ are the pre- and thermal strains; $\boldsymbol{\varepsilon}_f$ and $\boldsymbol{\varepsilon}_a$ are the strains in the frozen and active phases, respectively; Subscript M and T denote Mechanical and thermal strains, respectively.

For a prescribed thermomechanical cycle, the thermal and mechanical frozen fractions are different. The deformation of the mechanical pre-strain is received at temperature much higher than T_g , which can be frozen mostly as the temperature decreases lower than T_g . The thermal strain, however, is accumulated during the whole thermalmechanical process. The part of the thermal strain accumulated at $T > T_g$ can be frozen mostly as the temperature decrease to be lower than T_g , but the part of the thermal strain accumulated at $T < T_g$ can hardly be frozen. Consequently the overall constitutive equation for the polymer in a thermomechanical cycle can be determined by

$$\boldsymbol{\sigma} = \tilde{\mathbf{L}} (\boldsymbol{\varepsilon} - \boldsymbol{\varepsilon}_f^M - \boldsymbol{\varepsilon}_f^T) = \tilde{\mathbf{L}} [\boldsymbol{\varepsilon}^{pre} (1 - \Phi_f^M) + \boldsymbol{\varepsilon}^T (1 - \Phi_f^T)], \quad (11)$$

where Φ_f^M and Φ_f^T are respectively mechanical and thermal frozen fractions, which can be determined by Eq. (6) or (7). Variable $\tilde{\mathbf{L}}$ can be determined by Eq. (8).

Parameters determination and modeling results

Here we determine the material parameters according to the experimental results carried out by Liu et al. [15]. The test specimens are a commercial thermoset epoxy system, DP5.1 supplied by Composite Technology Development (CTD), Inc. The glass transition peak at approximately $T_g = 343$ K, with a drop in storage modulus of approximately two orders of magnitude from $T_l = 273$ K to $T_h = 358$ K.

The uniaxial free strain recovery curve was used to derive Φ_f . The mechanical frozen strain as a function of the temperature can be determined by the total recovery strain subtracted by the thermal recovery strain as shown in Fig.2. Fig. 3 presents the total recovery strain and the mechanical recovery strain at

$\varepsilon^{pre} = \pm 9.1\%$, and the thermal recovery strain. The mechanical frozen fraction, Φ_f , can be determined by the mechanical recovery strain divided by the pre-strain and fitted by Eq. (7). Fig. 4 shows the fitting results. The mechanical fitting strain at constant heating rate is expressed as

$$\Phi_f(T) = \varepsilon^{pre} \alpha \exp[-K(T_g/T - \tau)^m]. \quad (12)$$

The fitting coefficients for the expression of mechanical frozen fraction were listed in Table 1.

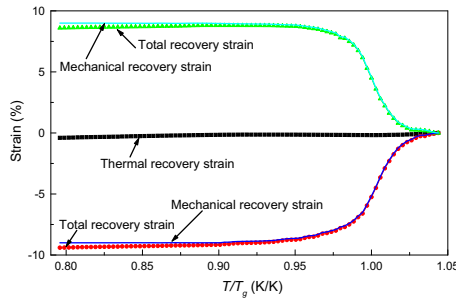


Figure 3: Different strains vs. temperatures.

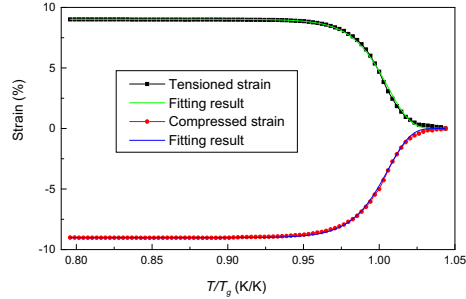


Figure 4: Experimental frozen strains and fitting results.

Comparing with the large mechanical pre-strain, the contribution of the thermal strain to the frozen strain of SMPs is limited. However, the mechanical pre-strain will be frozen mostly at low temperature (see Fig. 3). The strain recovery response during heating process is greatly dependent on the thermal strain. Hence, the character of the thermal strain for SMPs during cooling/heating process must be considered independently. The total thermal strain can be experimentally measured. The frozen thermal strains at any temperature can be calculated by Eq. (6) or (7), and then the unfrozen thermal strain is received by subtracting the frozen thermal strains from the total thermal strain. According to the fitting parameters listed in Table 1, the total-, frozen- and unfrozen-thermal strains versus temperature decrease are shown in Fig. 5. As the temperature is higher than the frozen transition temperature, nearly no thermal strain is frozen, and the absolute increasing rate of the unfrozen strain is nearly coincident with that of the total thermal strain. As the temperature is in the frozen transition zone, both the existed and newly developed thermal strains will be frozen mostly. The absolute increasing rate of the frozen thermal strains is even higher than that of the total thermal strain. As the temperature is much lower than the frozen transition temperature, the frozen thermal strain will reach to a constant value and the newly developed thermal strain can hardly be frozen.

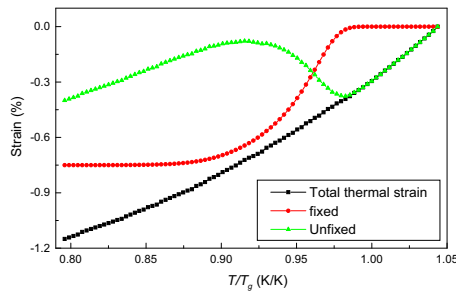


Figure 5: Thermal strains vs. temperatures.

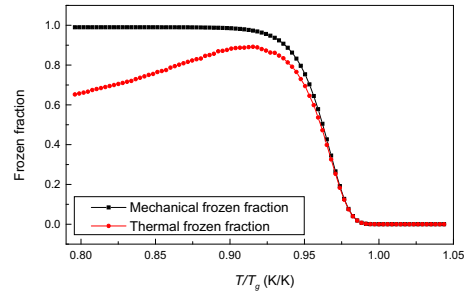


Figure 6: Mechanical and thermal frozen fractions vs. temperatures.

Fig. 6 provides the mechanical frozen fraction and thermal frozen fraction as a function of the temperature. The mechanical frozen and unfrozen strains keep nearly constant values at low temperature and cannot provide an initial shape recovery stress. The thermal unfrozen strain, however, is dependent on the shape retaining temperature, T_l , which indicates that suitable T_l -value should be considered for SMPs to receive enough recovery stress in the engineering application.

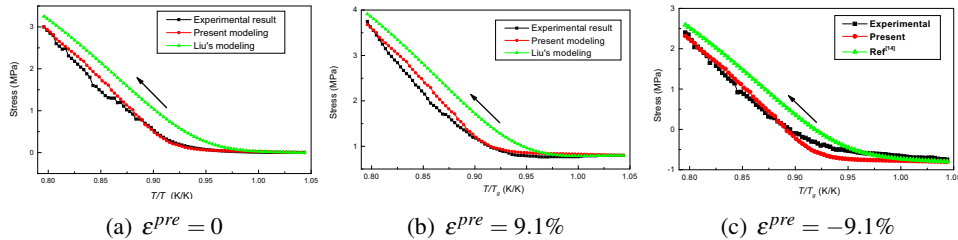


Figure 7: Modeling results of the stress responses of SMPs under different pre-strain constraint conditions.

Fig. 7 shows the experimental and modeling results of the stress responses of SMPs under different pre-strain constraint conditions. The experiment was carried out by Liu et al [15] and their modeling result was also provided as a comparison. The present predicting curves are not ideally smooth due to the effect of the thermal strain carried out by the experiment. However, the results are more close to the experimental values than that proposed by Liu et al. The critical point is that the frozen retardant time was considered in the present model, but Liu et al did not consider such factor. If we compare the cooling and heating experimental results as shown in Fig. 2 and Fig. 7, respectively, it is clear that the significantly different frozen transition temperatures can be found during heating/cooling process. Consequently, although both the frozen fraction calculated by the present model and

Liu's model is coincident with the experimental values, the predicting results of the stress recovery responses are significantly different.

Conclusions

The shape retaining and stress recovery response are critical for SMPs working as a kind of functional materials. In this study, a new constitutive model was proposed to predict the thermomechanical response of SMPs under different pre-strain constraint conditions. The behaviors of the thermal-strain frozen fraction and mechanical-strain frozen fraction as a function of the temperature are compared. The frozen retardant time of SMPs at constant cooling/heating rate is considered in the constitutive model. The predicting result by the new model exhibits more agreeable with the experimental values than that by the other models.

References

1. Lendlein, A.; Kelch, S. (2001): Shape-memory polymers. *Angew Chem Int. Ed.*, 41:2034-2057.
2. Murayama, Y.; Vinuela, F.; Tateshima, S.; Song, J.K.; Gonzalez, N.R.; Wallace, M.P. (2001): Bioabsorbable polymeric material coils for embolization of intracranial aneurysms: a preliminary experimental study. *J Neurosurg*, 94(3):454-463.
3. Robin, J.; Martinot, S.; Curtil, A.; Vedrinne, C.; Tronc, F.; Franck, M.; Champsaur, G. (1998): Experimental right ventricle to pulmonary artery discontinuity: outcome of polyurethane valved conduits. *J Thorac Cardiovasc Surg*, 115(4):898-903.
4. Wabers, H.D.; Hergenrother, R.W.; Coury, A.J.; Cooper, S.L. (1992): Thrombus deposition on polyurethanes designed for biomedical applications. *J Appl Biomater*, 3(3):167-76.
5. Lake, M.S.; Munshi, N.A.; Tupper, M.L. (2001): Application of elastic memory composite materials to deployable space structures. *AIAA Paper*, No. 2001-4602.
6. Mark, S.L.; Hazelton, C.S. (2002): Development of coilable longerons using elastic memory composite material. *AIAA Paper*, No. 2002-1453.
7. Francis, W.; Lake, M.S.; Mallick, K. (2003): Development and testing of a hinge/actuator incorporating elastic memory composites. *AIAA Paper*, No. 2003-1496.
8. Lee, A.P.; Fitch, J.P. (2000): Micro devices using shape memory polymer patches for mated connections. United States Patent 6,086,599.
9. Lee, A.P.; Northrup, M.A.; Ciarlo, D.R.; Krulevitch, P.A.; Bennett, W.J. (2000):

- Release mechanism utilizing shape memory polymer material. United States Patent 6,102,933.
10. Bhattacharyya, A.; Tobushi, H. (2000): Analysis of the isothermal mechanical response of a shape memory polymer rheological model. *Polymer Engineering and Science*, Vol. 40, No.12, pp. 2498-1676.
 11. Rao, I.J. (2002): Constitutive modeling of crystallizable shape memory polymers. *In the proceedings of SPE-ANTEC*, pp. 1936-1940.
 12. Rao, I.J.; Rajagopal, K.R. (2001): A study of strain induced crystallization in polymers, *International Journal of Solids and Structures*, Vol. 38, pp. 1149-1167.
 13. Rao, I.J.; Rajagopal, K.R. (2002): A thermodynamic framework to study crystallization in polymers. *ZAMP*, Vol. 53, pp. 365-406.
 14. Liu, Y.P.; Gall, K.; Martin, L. et al. (2006): Thermomechanics of shape memory polymers: Uniaxial experiments and constitutive modeling. *Int. J. Plasticity*, 22:279-313.
 15. Tobushi, H.; Okumura K.; Hashimoto, T. et al. (2001); Thermomechanical constitutive model of shape memory polymer. *Mechanics of Materials*, 33:545-554.
 16. Avrami, M.J. (1940): Kinetics of phase change II: Transformation-time relations for random distribution of nuclei *Chem Phys*, 8:212.
 17. Ozawa, T. (1971): Kinetics of non-isothermal crystallization *Polymer*, 12:150.
 18. Mori, T.; Tanaka, K. (1973): Average Stress in Matrix and Average Energy of Materials with Misfitting Inclusions, *Act. Metall*, 21:571-574.
 19. Eshelby, J.D. (1957): The Determination of the Elastic Field of an Ellipsoidal Inclusion and Related Problems, *Proceedings of the Royal Society*, London, Series A, 240:367-396.
 20. Eshelby, J.D. (1959): The Elastic Field Outside an Ellipsoidal Inclusion. *Proc. Roy. Soc.*, A252:561-569.

